Double-modified oncolytic adenovirus armed with a recombinant interferon-like gene enhanced abscopal effects against malignant glioma

Shan Jiang[†],[©], Hui-Hui Chai[†], Xian-Long Fang[†], Hou-Shi Xu, Tian-Wen Li, Qi-Sheng Tang, Jin-Fa Gu, Kang-Jian Zhang, Xin-Yuan Liu, Zhi-Feng Shi, Xue-Ping Cao, Zan-Yi Wu, and Liang-Fu Zhou

National Center for Neurological Disorders, Shanghai, China (S.J., H.-S.X., T.-W.L., Q.-S.T., Z.-F.S., H.-H.C., L.-F.Z.); Department of Neurosurgery, Huashan Hospital, Fudan University, Shanghai, China (S.J., H.-S.X., T.-W.L., Q.-S.T., Z.-F.S., H.-H.C., L.-F.Z.); Neurosurgical Institute, Fudan University, Shanghai, China (S.J., H.-S.X., T.-W.L., Q.-S.T., Z.-F.S., H.-H.C., L.-F.Z.); Shanghai Clinical Medical Center of Neurosurgery, Shanghai, China (S.J., H.-S.X., T.-W.L., Q.-S.T., Z.-F.S., H.-H.C., L.-F.Z.); Academician Expert Workstation of Fengxian District, Shanghai Yuansong Biotechnology Limited Company, Shanghai, China (X.-P.C., X.-L.F., J.-F.G., K.-J.Z.); Institute of Smart Biomedical Materials, School of Materials Science and Engineering, Zhejiang Sci-Tech University, Hangzhou, China (K.-J.Z.); State Key Laboratory of Cell Biology, Institute of Biochemistry and Cell Biology, Shanghai Institutes for Biological Sciences, Chinese Academy of Sciences, Shanghai, China (X.-Y.L.); Xinyuan Institute of Medicine and Biotechnology, Zhejiang Sci-Tech University, Hangzhou, China (X.-Y.L.); Department of Neurosurgery, The First Affiliated Hospital of Fujian Medical University, Fuzhou, Fujian, China (Z.-Y.W.)

Corresponding Authors: Zanyi Wu, No.20 Cha-Zhong Road, Fuzhou City, Fujian Province, China (kirby98@126.com); Xue-ping Cao, No.1588, Huhang Road, Fengxian District, Shanghai, China (caoxueping@yuansongbio.com).

[†]These authors contributed equally to this work.

Abstract

Background.   The development of new therapies for malignant gliomas has been stagnant for decades. Through the promising outcomes in clinical trials of oncolytic virotherapy, there is now a glimmer of hope in addressing this situation. To further enhance the antitumor immune response of oncolytic viruses, we have equipped a modified oncolytic adenovirus (oAds) with a recombinant interferon-like gene (YSCH-01) and conducted a comprehensive evaluation of the safety and efficacy of this modification compared to existing treatments.

Methods.   To assess the safety of YSCH-01, we administered the oAds intracranially to Syrian hamsters, which are susceptible to adenovirus. The efficacy of YSCH-01 in targeting glioma was evaluated through in vitro and in vivo experiments utilizing various human glioma cell lines. Furthermore, we employed a patient-derived xenograft model of recurrent glioblastoma to test the effectiveness of YSCH-01 against temozolomide.

Results.   By modifying the E1A and adding survivin promoter, the oAds have demonstrated remarkable safety and an impressive ability to selectively target tumor cells. In animal models, YSCH-01 exhibited potent therapeutic efficacy, particularly in terms of its distant effects. Additionally, YSCH-01 remains effective in inhibiting the recurrent GBM patient-derived xenograft model.

Conclusions.   Our initial findings confirm that a double-modified oncolytic adenovirus armed with a recombinant interferon-like gene is both safe and effective in the treatment of malignant glioma. Furthermore, when utilized in combination with a targeted therapy gene strategy, these oAds exhibit a more profound effect in tumor therapy and an enhanced ability to inhibit tumor growth at remote sites.

Key Points

- YSCH-01 is safe and effective for malignant gliomas in vitro and in vivo.
- Carrying recombinant interferon-like genes can improve remote tumor-killing effect.
- YSCH-01 performs superior efficacy in recurrent GBM PDX.

Importance of the Study

Armed with interferon-like gene, YSCH-01 has further enhanced the efficacy of oncolytic virotherapy for malignant gliomas. In combination with in vitro and in vivo experiments, YSCH-01 shows unique remote tumor inhibition effect, especially for recurrent GBM patients, and may have superior long-term survival benefits.

Glioblastoma (GBM), which accounts for 55% of all primary malignant brain tumors, is characterized by its highly malignant nature, poor prognosis, and tendency to recur.[1,2] Newly diagnosed GBM patients have a median survival time of less than 20 months, with a 5-year survival rate of only 5%.[3] The primary treatment approaches for GBM include surgical resection and postoperative chemoradiotherapy, while alternative methods encompass targeted therapy, immunotherapy, and tumor electric field therapy.[4–6] Despite these efforts, the survival time of GBM patients remains unacceptably static, and the development of novel drugs faces substantial obstacles and a high failure rate. Furthermore, recurrent GBM lacks proven interventions and standardized therapy. Consequently, GBM's 5-year survival rate has exhibited meager progress over the past 3 decades, highlighting a pressing need for effective interventions.

Notably, the use of oncolytic viruses has shown significant efficacy in treating recurrent GBM.[7–9] The oncolytic virus Delytact (G47Δ), in particular, has obtained conditional approval for market release in Japan based on its impressive survival benefits, observed in a Phase II clinical trial. Following OV treatment, the median overall survival for recurrent glioblastoma was 20.2 months.[10]

OVs are viruses that occur naturally or are genetically modified to have the ability to replicate within tumor cells. Their antineoplastic efficacy stems primarily from their direct tumor-killing effect and their indirect antitumor immunity effect.[11] OVs can cause direct lysis of tumor cells by propagating within them. Additionally, by recruiting immune cells to the site of infection and exposing tumor antigens subsequent to tumor cell lysis, oncolytic virus therapy can indirectly alter the local tumor immune environment from "cold" to "hot," triggering an antitumor immune response.[12,13] This effect has been implicated as a possible reason for long-term survival in cases of recurrent glioblastoma multiforme (GBM) in clinical trials.[9,14] However, the immune environment also plays a role in clearing OVs. Therefore, accurately regulating the tumor immune environment in relation to OVs at various stages while facilitating effective viral replication and inducing long-term antitumor immune effects simultaneously has become an important direction for the next generation of OV therapy.

We have developed a cancer-targeting gene-viro-therapy strategy by creating an oncolytic adenovirus (named YSCH-01) that incorporates an interferon-like immune anticancer gene (L-IFN). Based on our previous study, we optimized a new recombinant interferon termed sIFN-I, which was verified to possess a better affinity for IFNAR1 and exhibited an extended half-life in mice against solid tumors.[15] Therefore, we developed an interferon-like immune anticancer gene (L-IFN) carried by a double-regulated replicating human adenovirus type 5. The inserted L-IFN gene replicates within the tumor cells, along with the viral vector. Consequently, a substantial amount of L-IFN protein is expressed within the tumor cells and secreted into the extracellular space. By administering the L-IFN drug with the OV through direct injection, our cancer-targeting gene-viro-therapy strategy capitalizes on an optimal time window for virus replication and therapeutic gene expression (L-IFN). We have conducted comprehensive in vitro and in vivo studies to validate the safety and efficacy of YSCH-01. These investigations strongly support our modification strategy, which exhibits enhanced potential for achieving an impactful oncolytic effect.

Materials and Methods

Ethics Statement

All human samples were collected with the approval of China Ethics Committee of Registering Clinical Trials (ChiECRCT20190201). All patient information and tumor samples were obtained with the informed consent of the patient before surgery.

Cell Culture

THE glioma cells included U-138 MG, LN-18, T-98G, LN-229, U-118 MG, U-87 MG, HFF-1, and U-87 MG-Luc were purchased from National Collection of Authenticated Cell Cultures, Shanghai, China, which also provides STR profiling information. All glioma cells were maintained in DMEM containing 10% FBS, except for U-138 MG which required an additional 1% non-essential amino acids. In addition, HFF-1 cell line was maintained in DMEM medium supplemented with 15% FBS. The culture conditions for all cells were 37°C and 5% CO_2.

Establishment of Oncolytic Adenoviruses

The oncolytic adenovirus utilized in our study was developed by Shanghai Yuansong Biotechnology Co, Ltd. and is currently being used in a clinical trial (NCT05180851) for the treatment of various solid tumors, including breast cancer, lung cancer, and melanoma. The OncoMul-V2 used the human adenovirus type 5 (Ad5) genome as the backbone.[16] Its E1A gene was deleted with a 24-bp sequence,[17] and its wild-type promoter was replaced with survivin promoter. The YSCH-01 was constructed by inserting the complete expression cassette of the L-IFN gene, a modified type I interferon gene, between the packaging signal region of

Ad5 and the survivin promoter based on the structure of OncoMul-V2. The gene sequence of L-IFN was synthesized by multiplex PCR technique (General Biosystems, Anhui, China), and its expression was controlled by a human cytomegalovirus (HCMV) promoter.

Detection of the L-IFN Proteins in Supernatant

Briefly, GBM patient-derived primary tumor cells were seeded in 24-well plates at a density of 1×10^5 cells per well. After overnight incubation, those cells were treated with vehicle or infected with Mock (PBS), OncoMul-V2, replication-defective YSCH-01 or YSCH-01 at 1 ifu/cell. After 72 hours, the L-IFN concentration in the cell culture supernatant was measured using a commercially available human IFNα ELISA assay kit (#41100, PBL Assay Science, Piscataway, NJ, USA).

In Vitro Cytotoxicity Assay

Cells were plated on 96-well plates at a density of 4×10^3 cells per well except U-87 MG at 1×10^3 cells per well. After overnight incubation, those cells were infected with 10 μL oAds at different MOIs. Cell viability was determined 4 days after viral infection by Cell Counting Kit-8 (CCK8) assay (#40203ES80, Yeasen Biotechnology, Shanghai, China), and the IC50 value was calculated with GraphPad Prism (ver. 8.0). All assays were performed at least 3 times.

In Vivo, Study to Evaluate the Antitumor Efficacy of OVs

Female Balb/c-nude mice at 4–5 weeks of age were purchased from Lingchang Biotechnology Co., Ltd. (Shanghai, China). The mice were housed in a specific pathogen-free grade animal house, and the environment was controlled at a temperature of 20 to 26°C, a humidity level of 40% to 70%, and a light cycle consisting of 12 hours of light, followed by 12 hours of dark. All animal experiments were carried out in accordance with the National Institute of Health Guide for the Care and Use of Laboratory Animals.

Briefly, as for cell-derived xenograft (CDX) tumors, aliquots of 2×10^6 glioma cells were subcutaneously (s.c.) injected into both flanks of the mice. When the tumor volume reached approximately 120 mm^3, the animals were divided and received treatment into one side of the tumors. The tumor growth was measured every 3 days. The experiment was terminated when the mean tumor volume in the Vehicle group reached about 2000 mm^3.

For the intracranial glioma model, the subcutaneous U-87 MG-Luc tumor was removed and cut into tumor masses with a diameter of 0.5 to 1 mm. A tumor mass was transplanted intracranially (i.c) into the right lobe of nude mouse. After 7 days, the mice received treatments and the bioluminescence imaging (BLI) was performed (Viewworks, KOREA) every 7 days for 4 times.

For the Patient-derived tumor xenograft (PDX) model, human patient tissue samples were collected under the approval of China Ethics Committee of Registering Clinical Trials (ChiECRCT20190201). The recurrent glioblastoma tumor masses, which had been acclimatized to the fifth generation in immunodeficient mice, were transplanted on the right flank of nude mice. When the tumor volume reached about 150 mm^3, the nude mice received treatment.

Detection of Apoptosis

Glioma cells were plated on 12-well plates at a density of 2×10^5 cells per well. Following an overnight incubation, the cells were subjected to vehicle or infected with OVs at 10 MOI (LN-18, LN-229) in triplicate. After 48 hours, the cells were harvested for apoptosis detection (#40302ES60, Yeasen). The FACS assay was then performed with a flow cytometer (Agilent Technologies).

Western Blot Analysis of Cell Death-Related Proteins

Glioma cells were plated on 6-well plates at a density of 4×10^5 cells per well. After overnight incubation, the cells were treated with vehicle or infected with OVs at 10 MOI (LN-18, LN-229). Briefly, after 48 hours later, aliquots of total 20 ug protein mixture were separated and transferred to polyvinylidene fluoride (PVDF) membranes. Protein bands were visualized using a chemiluminescence system (Tanon, Shanghai, China) in combination with enhanced chemiluminescence (ECL) detection reagents (#36208ES60, Yeasen). The primary antibodies included: A-caspase 3 (#19677-1Ap, Proteintech, Wuhan, China), a-caspase 9 (#10380-1Ap, Proteintech), a-poly (ADP-ribose) polymerase (PARP) (#9542, Cell Signaling, Danvers, MA, USA), a-LC3B (#2775s, Cell Signaling), and a-GAPDH (#CY6717, Abways). The secondary antibody (#33101ES60, Yeasen) was obtained from Yeasen Biotechnology Co., Ltd. (Shanghai, China).

Staining of Tumor Tissue Sections

In subcutaneously CDX models, tumors were collected 13 days after the initial drug administration. The tissues were fixed and embedded in paraffin, cut into 3 um sections. For histological analysis, the sections were deparaffinized and stained with hematoxylin and eosin (H&E). Immunohistochemical analysis was performed on other sections. The primary antibodies used were a-Ki67 (#ab15580, abcam, Cambridge), a-CD45 (#ab208022, abcam), and a-CD31 (#ab182981, abcam). The HRP polymer secondary antibody and DAB reagents were obtained from the En Vision kit (#K5007, Dako, Denmark). Hematoxylin was used as a counterstain. Furthermore, additional sections underwent the TUNEL assay with In Situ Cell Death Detection kit (#1168479591).

Toxicity and Pharmacokinetics Evaluation of YSCH-01 Intracranial Injection

Four to five-week-old hamsters were purchased from Beijing Vital River Lab Animal Technology Co., Ltd. and housed in a W-free environment, following a

protocol approved by the Institutional Animal Care and Use Committee. Prior to the experiments, the hamsters were acclimatized for 1–2 weeks.

To assess toxicity of YSCH-01, Syrian hamsters were randomly assigned into 3 groups at random. Each group consisted of 4 male and 4 female hamsters. After anesthetizing, intracranial injections of the drugs were performed using a stereotaxic apparatus. Body weight were measured throughout the experiment. Brain tissues and major organs from hamsters treated with the drug were collected. Additionally, peripheral blood samples were collected from hamsters to analyze hemogram and liver function.

To quantify the copies of YSCH-01 vector, DNA was extracted from the samples using the tissue DNA extraction kit (#DE0596B, Emerther, China). Blood DNA was directly extracted from 200 µL thawed samples using blood genome extraction kit (#DE17002, Emerther) and the automatic nucleic acid extractor. The copies of the YSCH-01 vector in the tissue or blood DNA were determined using real-time PCR with Probe qPCR Mix (#RR392A, TAKARA, Japan).

To determine the content of L-IFN in the right brain, the collected tissues at different time points were dissolved in PBS (1g in 4 mL), homogenized, and centrifuged at 12 000 rpm for 10 minutes at a low temperature. The supernatants were then used for quantification using a human IFNa ELISA assay kit.

Statistical Analysis

All the data were expressed as the mean ± standard deviations (SDs). GraphPad Prism (ver. 8.0) was utilized for charting and statistical analysis. Certain specific analyses were performed using a one-way analysis of variance (ANOVA) or Log-rank (Mantel-Cox) test. Statistical significance was considered at a *P*-value of < .05.

The details of methods can be found in Supplementary Materials.

Results

Modified oncolytic adenovirus armed with recombinant Type I interferon that specifically targets glioma cells and be safe in the Syrian hamster model.

To enhance the targeting and efficacy of the oncolytic adenovirus, we implemented genetic engineering from 2 perspectives: Modifying virus-specific initiation conditions and incorporating therapeutic genes. Initially, we modified the oncolytic adenovirus, named OncoMul-V2, by incorporating the survivin promoter and deleting 24 base pairs from the viral E1A genomic region (Figure 1A). These double modifications significantly improved the virus's targeting ability towards glioma cells and tissues. Our findings demonstrated that the IC50 of the modified virus on
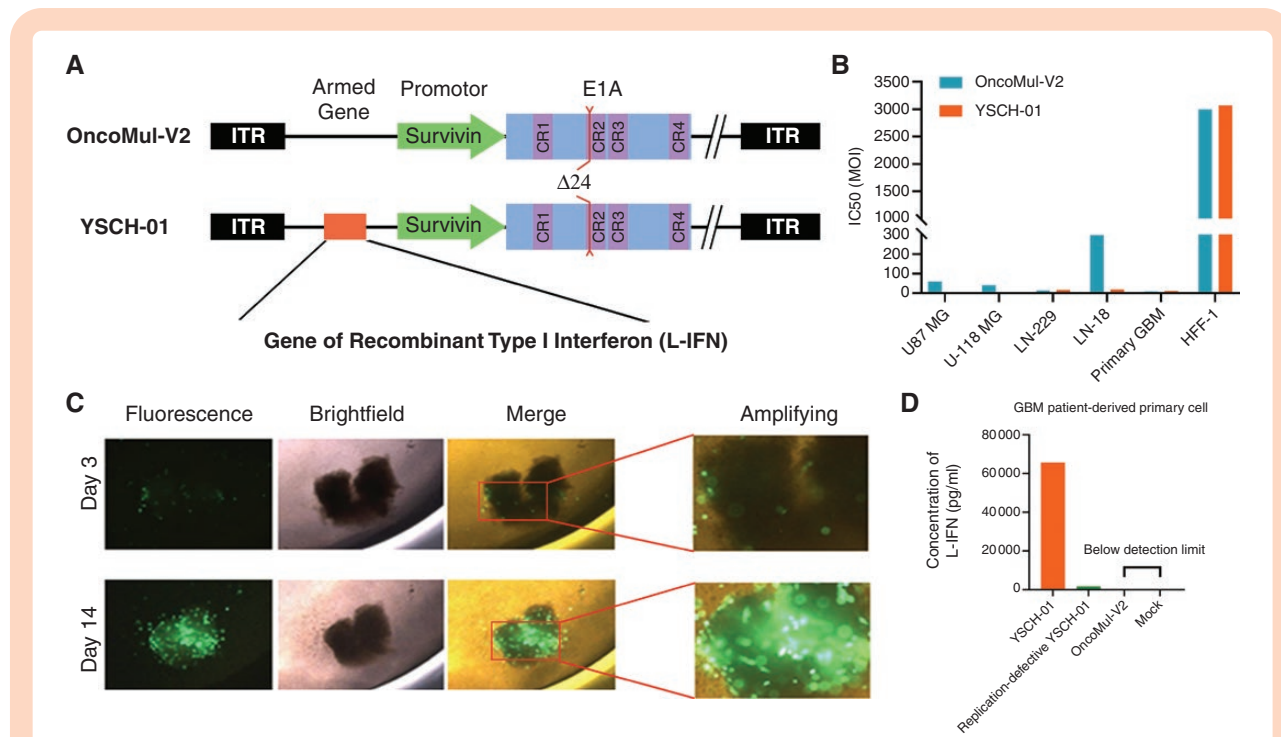

Figure 1. Modified oncolytic adenovirus armed with recombinant Type I interferon specifically targeted glioma cells. (A) Schematic representation of viral genetic modification. The upper represents OncoMul-V2 and the lower is YSCH-01. (B) Four glioma cell lines, one GBM patient-derived primary cell, and HFF-1 lines were, respectively incubated with the virus for 96 hours and cell viability assays were performed to evaluate IC50. (C) The representative images of 3D culture of patient-derived glioma tumor tissue administrated with modified oncolytic adenovirus carrying green fluorescent protein gene. (D) Concentration of L-IFN in supernatant of GBM patient-derived primary cell 72 hours after YSCH-01/Replication-defective YSCH-01/OncoMul-V2/Mock treatment.

human foreskin fibroblasts (HFF-1) cells was significantly higher compared to human glioma cell lines (U-87 MG, U-118 MG, LN-229, and LN-18) and GBM patient-derived primary tumor cell, indicating the safety of the modified oncolytic adenovirus on normal cells (Figure 1B and Supplementary Figure S1). In addition, we employed a 3D culture of patient-derived glioma tissue and found that the modified oncolytic adenovirus, labeled with the green fluorescent protein gene, expressed itself in tumor tissue, reaching its peak fluorescence intensity on the 14th day (Figure 1C and Supplementary Figure S2). Subsequently, we further equipped OncoMul-V2 with a gene encoding a novel recombinant Type I interferon (L-IFN), previously designed by our team (named YSCH-01) (Figure 1A). This recombinant L-IFN exhibited a greater affinity for the

IFNAR1 chain of the IFN1 receptor, leading to stronger IFN1 signaling and expression of IFN-inducible genes in human cells.[15] As the virus infected and proliferated, the L-IFN gene was transcribed, translated, and released into the extracellular fluid in GBM patient-derived primary tumor cells (Figure 1D). Our triple modifications have endowed the adenovirus with enhanced targeting towards glioma and increased oncolytic potency.

Considering that adenoviruses replicate 1000-fold less efficiently in mouse cells than in human cells,[18] we conducted intracranial injections of YSCH-01 (0.25×10^9/ 1×10^{10} VP per hamster) into the brains of Syrian hamsters. Syrian hamsters, one of the only 2 small mammals that support efficient adenovirus replication,[19–22] were chosen to precisely evaluate the safety of the virus (Figure 2A).
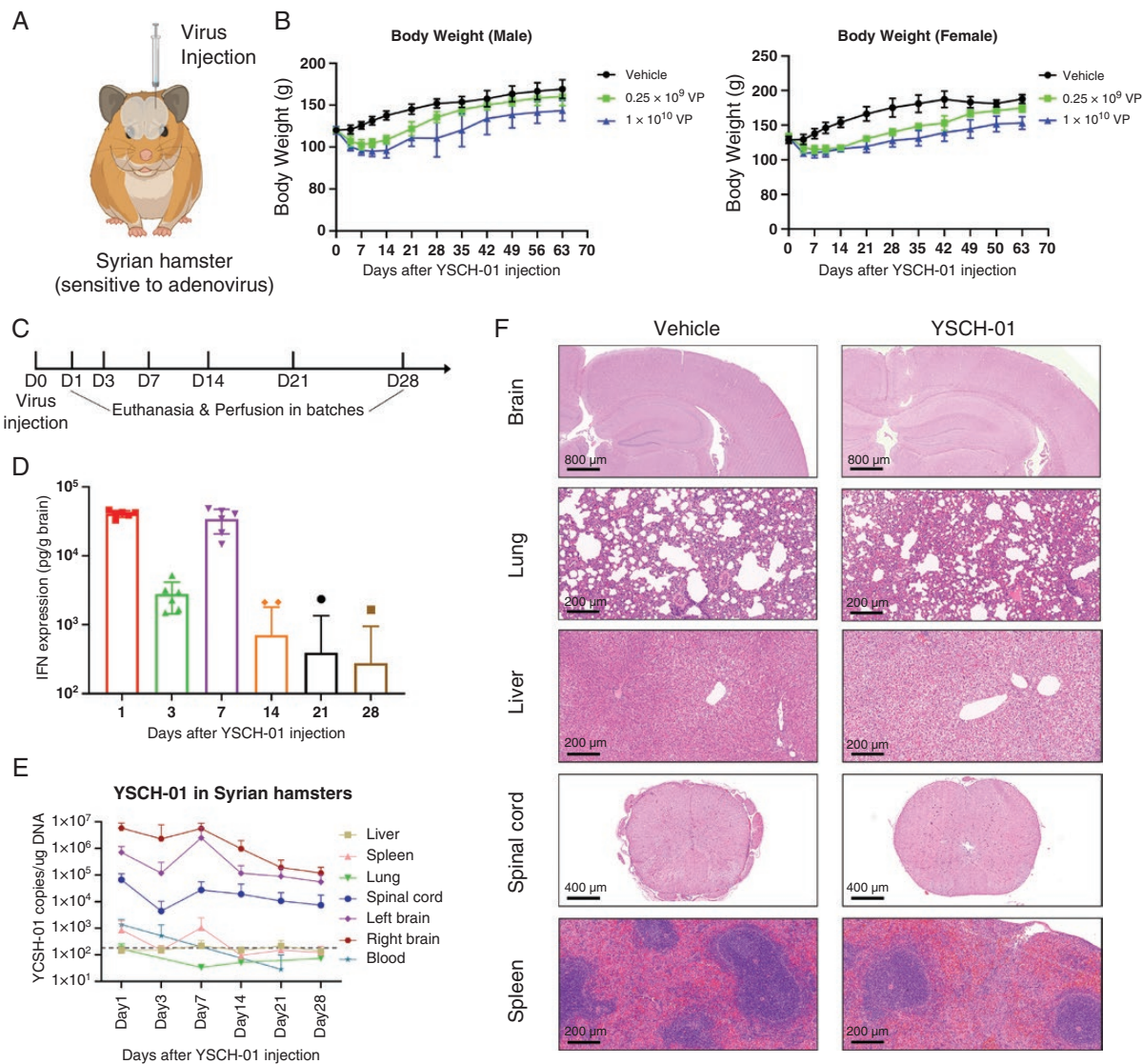

Figure 2. Syrian hamster model verified the safety of intracranial injection of YSCH-01. (A) Syrian hamsters permitted adenovirus multiplicities of infection. YSCH-01 was injected into healthy hamsters' hemiencephalon. (B) The body weight of male ($n = 4$) and female ($n = 4$) hamsters after virus injection. (C-E) We injected YSCH-01 into a group of healthy hamsters and perfused hamsters ($n = 6$) in batches to detect L-IFN expression and YSCH-01 copies in brain and peripheral organs. (F) The representative HE staining images of organ slices after YSCH-01 treatment.

Following virus injection, the hamsters exhibited a temporary decrease in body weight, which gradually returned to normal levels (Figure 2B). Additionally, time-series experiments were conducted to examine the viral pharmacokinetics in the brain and major peripheral organs post-injection (Figure 2C and Supplementary Figure S3). The expression of L-IFN peaked on the first day after injection and then gradually decreased, only to increase again on the 7th day due to virus replication. Subsequently, the expression levels gradually declined, with only a few detectable samples remaining after the 14th day (Figure 2D). Similar trends were observed in the YSCH-01 genomic copy numbers in brain tissue, major peripheral organs, and blood (Figure 2E). Collectively, the Syrian hamster model confirmed the replication capacity of the virus and the efficacy of L-IFN gene expression following intracranial administration.

YSCH-01 had better tumor-killing effectiveness in glioma subcutaneous xenografts and a distal tumor inhibition effect.

To validate the therapeutic efficacy of YSCH-01, we utilized different glioma cell lines to establish subcutaneous xenograft models in nude mice. For the LN-229 xenograft model, LN-229 cells were subcutaneously injected into the bilateral flank of nude mice. Once the tumors reached approximately 100 mm^3 (24 days later), the mice were randomly divided into 3 groups and injected with different drugs (vehicle, OncoMul-V2, YSCH-01) into unilateral tumors at a dosage of 1×10^{10} VP/mouse. Tumor volumes were measured every 3 days. After 27 days of virus injection, the mice were euthanized for further analysis (Figure 3A). Our results demonstrated that YSCH-01 significantly reduced the tumor volumes on both the injection and contralateral sides. In contrast, treatment with OncoMul-V2 only mildly
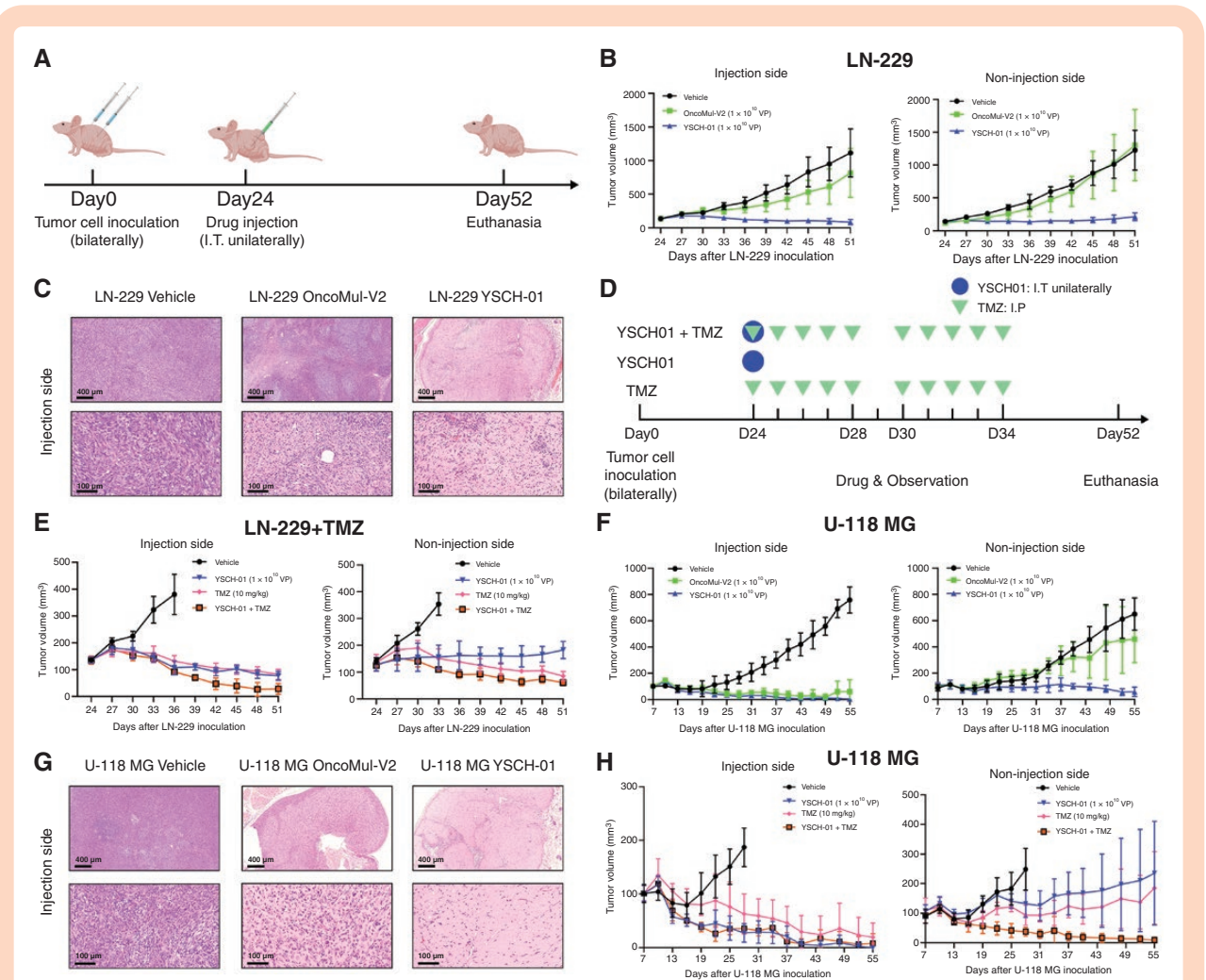

Figure 3. Growth suppression of glioma subcutaneous xenografts by intratumoral injection of YSCH-01. (A) Flow diagram of experiments to test the efficacy of YSCH-01 in subcutaneous LN-229 xenograft immunodeficient mice models. (B) The time plot of Balb/c-nude mice's LN-229 tumor volumes after drug treatment (Vehicle, OncoMul-V2, YSCH-01, *n* = 5). (C) The representative HE staining images of LN-229 xenograft tumor sections (injection site) 13 days after drug treatments. Scale bar (upper 400 μm; nether 100μm). (D) Flow diagram of experiments to test the efficacy of YSCH-01 in subcutaneous U-118 MG xenograft immunodeficient mice models. (E) The time plot of Balb/c-nude mice's U-118 MG tumor volumes after drug treatment (Vehicle, OncoMul-V2, YSCH-01). (F) The representative HE staining images of U-118 MG xenograft tumor sections (injection site) 13 days after drug treatments. Scale bar (upper 400 μm; nether 100 μm). Tumor volume = (long axis × minor axis^2)/2.

suppressed the growth of the injected side tumor, without affecting the contralateral side (Figure 3B). Histological examination of tumor sections stained with HE revealed a significant reduction in the number of tumor cells and an increased infiltration of immune cells in tissues following YSCH-01 treatment (Figure 3C).

Similar experiments were also conducted using U-118 MG cells (Figure 3D). However, in contrast to the LN-229 mode, OncoMul-V2 exhibited a comparable tumor-killing effect to YSCH-01 at the injection site. Similar to the LN-229 model, OncoMul-V2 failed to suppress tumor growth in the contralateral site, whereas YSCH-01 consistently demonstrated excellent efficacy (Figure 3E). The findings from HE staining images were in line with the tumor growth observed in the animal model. In tumors located on the injection side, both OncoMul-V2 and YSCH-01 led to a reduction in tumor cells and increased immune infiltration. However, only YSCH-01 exhibited the ability to inhibit tumor cells (Figure 3F).

The oncolytic effect of YSCH-01 was further verified by intracranial glioma xenograft and patient-derived tumor xenograft.

To further confirm the efficacy of YSCH-01 in situ, we subcutaneously injected U-87 MG cells labeled with Luciferase into the unilateral hemisphere of nude mice.

Bioluminescence imaging was performed 8 days after tumor implantation to monitor tumor growth. The mice were then divided into 3 groups and treated with either a vehicle, a single dose of YSCH-01, or 3 doses of YSCH-01 (Figure 4A). Based on the fluorescence signal intensity and survival time, the results showed that a single injection of YSCH-01 significantly suppressed the growth of intracranial tumors and extended the survival time of the mice. While the 3-time repeat injections of YSCH-01 did not demonstrate a statistically significant advantage over the single injection (Figure 4B-D). Moreover, the inhibitory effect of YSCH-01 on distal tumors was confirmed in bilateral subcutaneous xenograft models (Figure 4E).

Furthermore, we aimed to investigate the oncolytic effect of YSCH-01 on heterogeneous tumor components. To achieve this, we established a recurrent glioblastoma patient-derived tumor xenograft by grafting cell suspensions derived from the patient's tumor samples into immunodeficient mice (Figure 4F). Notably, YSCH-01 exhibited significantly superior inhibition of tumor growth compared to treatment with TMZ (Figure 4G and Supplementary Figure S4A). Furthermore, YSCH-01 demonstrated sustained tumor suppression even after a single dose (Supplementary Figure S5B).
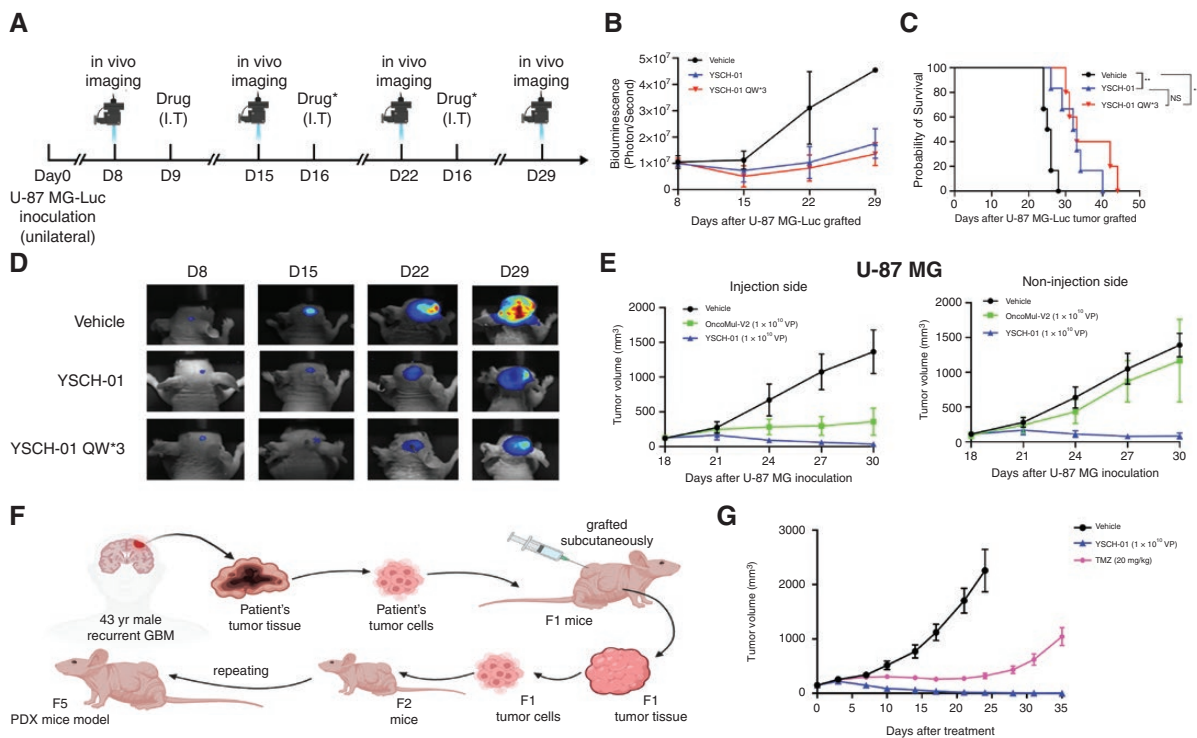

Figure 4. The oncolytic effect of YSCH-01 was further verified by intracranial glioma xenograft and patient-derived tumor xenograft. (A) Flow diagram of testing the efficacy of YSCH-01 in intracranial U-87 MG xenograft immunodeficient mice models. (B) Changes in tumor fluorescence intensity after drug administration (Vehicle, YSCH-01, triple injection of YSCH-01, $n = 6$ for each group). (C) Survival curves after drug administration (Vehicle, YSCH-01, triple injection of YSCH-01, $n = 6$ for each group) (Vehicle-YSCH-01: $P = .0029$; Vehicle-YSCH-01QW3: $P = .0014$; YSCH-01-YSCH-01QW3: $P = .2693$), n.s., not significant, $**P < .01$, Log-rank (Mantel-Cox) test. (D) The representative fluorescence imaging of the U-87 MG tumor. (E) The time plot of U-87 MG tumor volumes after drug treatment (Vehicle, OncoMul-V2, YSCH-01, $n = 5$ for each group) in subcutaneous xenograft immunodeficient mice models. (F) Flow diagram of establishing subcutaneous patient-derived tumor xenograft immunodeficient mice models. (G) The time plot of Balb/c-nude mice's PDX tumor volumes after drug treatment (Vehicle, TMZ, YSCH-01, $n = 10$ for each group).

The results of in situ CDX and subdermal patient-derived xenograft further confirmed the therapeutic efficacy of YSCH-01. The incorporation of dual promoter modifications on the adenovirus, along with the addition of the L-IFN gene, not only enhanced the killing effect on glioma models but also demonstrated a potential advantage over TMZ treatment for recurrent glioblastoma.

YSCH-01 increased tumor cell apoptosis and inhibited tumor proliferation and angiogenesis.

In this study, we have successfully validated the safety and efficacy of YSCH-01 as a potential treatment for malignant glioma, both in vitro and in vivo. Additionally, we conducted molecular biochemical investigations to elucidate the underlying mechanism of YSCH-01 in inhibiting tumor cells. Our findings demonstrated that YSCH-01 induced a significant increase in apoptosis in LN-18 human glioma cells, as evidenced by the results of flow cytometry (Figure 5A, B). However, this effect was less pronounced in
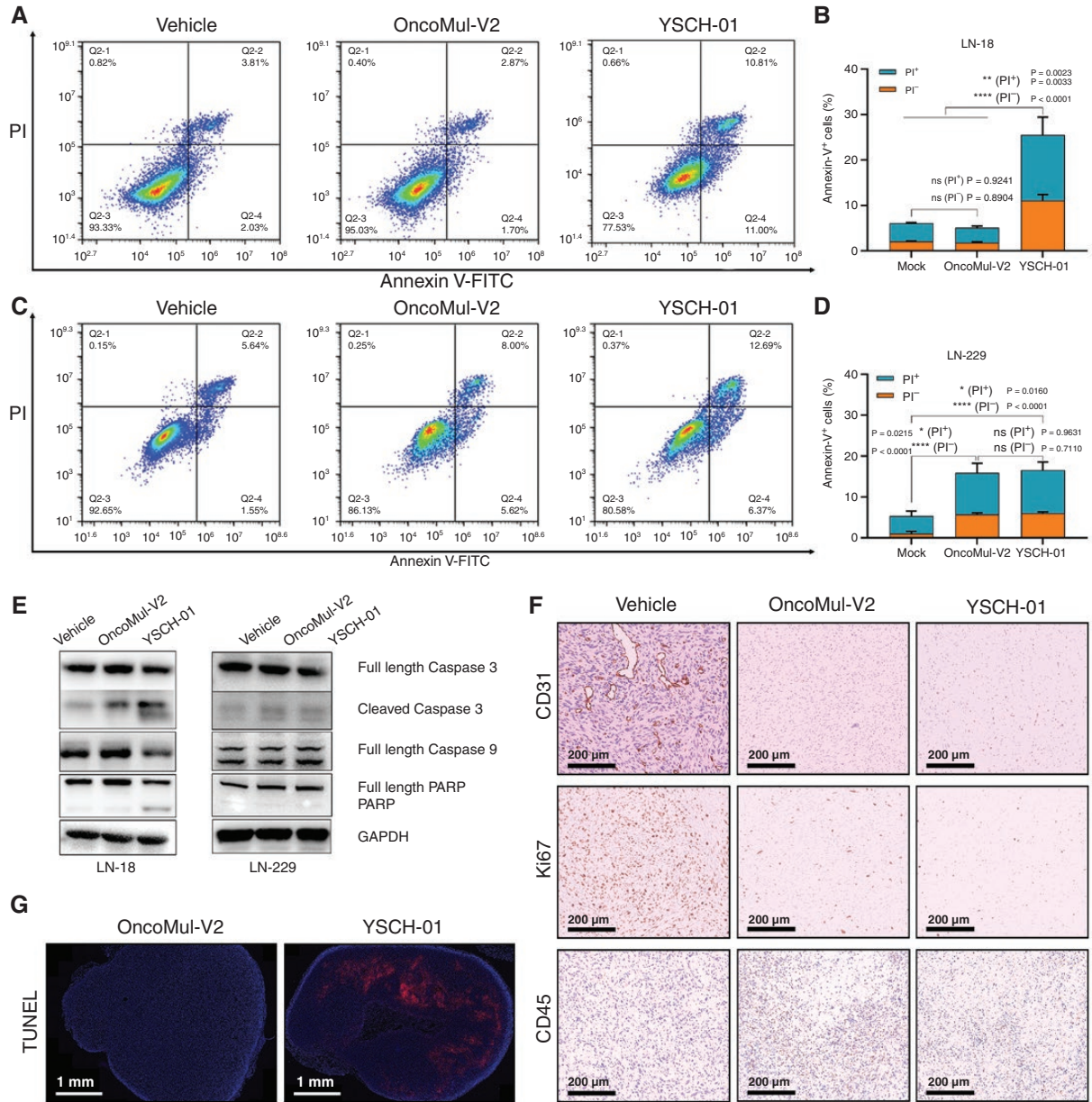

Figure 5. Exploration of the antitumor mechanism of YSCH-01. (A) Flow cytometry was used to detect the apoptosis of LN-18 tumor cells after treatment. (B) Under 10 MOI of virus treatments, the comparison of PI proportion among Annexin V-FITC-positive LN-18 cells. (C) Flow cytometry was used to detect the apoptosis of LN-229 tumor cells after treatment. (D) Under 10 MOI of virus treatments, the comparison of PI proportion among Annexin V-FITC-positive LN-229 cells. (E) Western Blot to detect makers related to cell apoptosis. (F) The representative immunohistochemical staining images of CD31, Ki67, CD45 in U-118 MG xenograft tumor sections 13 days after drug treatments. Scale bar, 100 μm. (G) The representative TUNEL immunofluorescent staining images of U-118 MG xenograft tumor sections 13 days after drug treatments. Scale bar, 1 mm. n.s., not significant, $*P < .05$, $**P < .01$, $***P < .001$, $****P < .0001$, one-way ANOVA followed by Tukey's multiple comparisons test.

LN-229 cells (Figure 5C, D). The results observations were consistent with the results obtained from Western Blot analysis. Specifically, YSCH-01 treatment led to the up-regulation of Cleaved Caspase 3 and PARP cleavage in LN-18 cells, indicating the activation of the apoptotic pathway. In contrast, these effects were not as prominent in LN-229 cells (Figure 5E). Furthermore, immuno-histochemical staining images taken 13 days after YSCH-01 injection demonstrated a significant reduction in Ki67-positive U-118 MG tumor cells (Figure 5F), indicating a suppression of tumoral cell proliferation. Additionally, YSCH-01 treatment resulted in a decrease in CD31-positive cells, suggesting a significant reduction in angiogenesis within the tumor tissue at the injection site (Figure 5F). There was an increase in CD45-positive tumor cells after oncolytic viral therapy (Figure 5F). The TUNEL tests confirmed that tumor cell apoptosis was enhanced following YSCH-01 treatment (Figure 5G).

Discussion

We conducted a preclinical investigation to evaluate the safety and efficacy of YSCH-01, an oncolytic adenovirus carrying a recombinant interferon-like protein (L-IFN), for the treatment of malignant glioma. In a Syrian hamster model sensitive to human adenovirus and in human tumor tissues, we demonstrated that the inclusion of the Survivin promoter along with a 24-bp deletion ensured tumor-specific infection and therapeutic safety of the oncolytic adenovirus. YSCH-01 exhibited superior long-term tumor inhibition and abscopal effect in both the CDX model of human glioma cell line and the recurrent-GBM PDX model.

The pharmacokinetics study of hamsters revealed 2 distinct peaks in the viral copy numbers of YSCH-01 and protein expression of L-IFN on days 1 and 7 following administration. These findings suggest that the fusion strategy of incorporating L-IFN therapeutic genes serves dual objectives by efficiently regulating local viral concentration while allowing ample space for viral replication. On one hand, as the YSCH-01 virus proliferates, the concentration of L-IFN concurrently increases at the first peak, impeding viral growth and maintaining a reasonable local concentration. On the other hand, as the first wave of L-IFN subsides, a permissive immune environment is established, promoting further virus replication, which ultimately leads to the observed peak on day 7. The Cancer Targeting gene-viro Therapy strategy regards OV as not only therapeutic drugs but also therapeutic vectors. The piggyback strategies employed in the development of the next-generation oncolytic viruses primarily encompass direct therapeutic gene targeting for tumor eradication and targeted synergistic collaboration with other immunotherapies. In the field of combination therapy, the research and development of oncolytic virus therapy are changing from simple combination administration to the design of specific target genes of oncolytic virus to specifically enhance the recruitment of CAR-T cells to solve the problem of insufficient abundance in the field of solid tumor treatment. For example, B7H3-targeted CAR-T cells were specifically recruited by an oncolytic adenovirus expressing CXCL11 for the treatment of glioblastoma, which significantly enhanced the recruitment and chemotaxis of CAR-T cells and improved TME while playing oncolytic effect.[23] As for direct therapeutic genes, they can be categorized into immune regulatory cytokines (such as GM-CSF,[24] IL-2,[25] L12,[26] and IL15[27]), chemokines (including CCL5,[28] CCL20[29]). Due to the limitation of viral vector capacity, how to select the best therapeutic gene becomes the main problem for this strategy. Although it is not possible to directly compare the advantages and defects of different gene-carrying strategies based on limited preclinical experiments, in our current study, we further modified the interferon gene (L-IFN) with the wild-type immune regulator to achieve significant in vivo efficacy of single gene carrying virus. At the same time, we also believe that with the precision modification of onboard therapeutic genes. Future oncolytic virotherapy also needs to evolve toward individualized drug delivery. How to find the appropriate biomarker to predict the response of patients to different types of modified oncolytic viral therapy will be a major problem to be solved in the future.

Understanding the mechanisms underlying the oncolytic effect of adenoviruses, particularly their indirectly induced antitumor immune response, is vital for promoting long-term survival in patients. Despite the notable distant effects observed with YSCH-01 in this study, a comprehensive exploration of the immune mechanism of this oncolytic virus is lacking due to the limited availability of suitable animal research models. It is worth noting that the replication ability of human adenovirus in rat or mouse cells is 1000 times lower than in human cells, and Syrian hamsters do not provide readily available glioma tumor models. To overcome this challenge, the literature describes the construction of an animal model using engineered Syrian hamster neural stem cells to investigate the immune mechanism of oncolytic adenovirus. Further elucidation of the immune mechanism of oncolytic virus therapy against tumors holds great promise in providing a theoretical foundation for the subsequent modification of oncolytic viruses.

Meanwhile, OncoMul-V2, a variant similar to the oncolytic adenovirus drug currently undergoing clinical trials, exhibited varying effects among different glioma cell lines. This observation suggests the presence of inherent differences in tumor cells, leading to heterogeneity in the effectiveness of oncolytic viruses within patients. Therefore, the identification of biomarkers that can accurately predict therapeutic efficacy becomes crucial and presents a significant clinical necessity and challenge. Consequently, in the design of clinical trials, it is imperative to place heightened emphasis on molecular profiling and analysis of patient tumor tissues.

Supplementary material

Supplementary material is available online at *Neuro-Oncology* (https://academic.oup.com/neuro-oncology)

Keywords

malignant glioma | oncolytic virus | preclinical study | recombinant interferon

Authorship statement

X.P.C. and Z.Y.W. designed the experiments and interpreted the results. S. J., H.H.C., and X.L.F. performed most of the experiments, with assistance from H.S.X., T.W. L., Q.S.T., and J.F.G. Meanwhile, S. J., H.H.C., and X.L.F. analyzed the data and generated the figures. S. Jiang, K.J.Z., and Z.F.S. wrote the manuscript. X.Y.L. and L.F.Z. reviewed the overall experimental process and revised the article. All the authors commented on the manuscript.

Conflict of interest statement

K.J.Z., X.L.F., J.F.G., and X.Y.L. hold ownership interests and own patents of YSCH-01 in Yuansong Biotechnology Co., Ltd. No potential conflicts of interest were disclosed by the other authors.

Data availability

The datasets used and analyzed during the current study are available from the corresponding author upon reasonable request.

References

1. Sung H, Ferlay J, Siegel RL, et al. Global cancer statistics 2020: GLOBOCAN estimates of incidence and mortality worldwide for 36 cancers in 185 countries. *CA Cancer J Clin.* 2021;71(3):209–249.
2. Chen F, Wendl MC, Wyczalkowski MA, et al. Moving pan-cancer studies from basic research toward the clinic. *Nat Cancer.* 2021;2(9):879–890.
3. Molinaro AM, Hervey-Jumper S, Morshed RA, et al. Association of maximal extent of resection of contrast-enhanced and non-contrast-enhanced tumor with survival within molecular subgroups of patients with newly diagnosed glioblastoma. *JAMA Oncol.* 2020;6(4):495–503.
4. Stupp R, Mason WP, van den Bent MJ, et al; European Organisation for Research and Treatment of Cancer Brain Tumor and Radiotherapy Groups. Radiotherapy plus concomitant and adjuvant temozolomide for glioblastoma. *N Engl J Med.* 2005;352(10):987–996.
5. Stupp R, Taillibert S, Kanner A, et al. Effect of tumor-treating fields plus maintenance temozolomide vs maintenance temozolomide alone on survival in patients with glioblastoma: A randomized clinical trial. *JAMA.* 2017;318(23):2306–2316.
6. Bagley SJ, Kothari S, Rahman R, et al. Glioblastoma clinical trials: Current landscape and opportunities for improvement. *Clin Cancer Res.* 2022;28(4):594–602.
7. Gállego Pérez-Larraya J, Garcia-Moure M, Labiano S, et al. Oncolytic DNX-2401 virus for pediatric diffuse intrinsic pontine glioma. *N Engl J Med.* 2022;386(26):2471–2481.
8. Fares J, Ahmed AU, Ulasov IV, et al. Neural stem cell delivery of an oncolytic adenovirus in newly diagnosed malignant glioma: A first-in-human, phase 1, dose-escalation trial. *Lancet Oncol.* 2021;22(8):1103–1114.
9. Desjardins A, Gromeier M, Herndon JE, et al. Recurrent glioblastoma treated with recombinant poliovirus. *N Engl J Med.* 2018;379(2):150–161.
10. Todo T, Ito H, Ino Y, et al. Intratumoral oncolytic herpes virus G47Δ for residual or recurrent glioblastoma: A phase 2 trial. *Nat Med.* 2022;28(8):1630–1639.
11. Sanmamed MF, Chen L. A paradigm shift in cancer immunotherapy: From enhancement to normalization. *Cell.* 2019;176(3):677.
12. Duan Q, Zhang H, Zheng J, Zhang L. Turning cold into hot: Firing up the tumor microenvironment. *Trends Cancer.* 2020;6(7):605–618.
13. Gujar S, Pol JG, Kroemer G. Heating it up: Oncolytic viruses make tumors "hot" and suitable for checkpoint blockade immunotherapies. *Oncoimmunology.* 2018;7(8):e1442169.
14. Todo T, Ino Y, Ohtsu H, Shibahara J, Tanaka M. A phase I/II study of triple-mutated oncolytic herpes virus G47 in patients with progressive glioblastoma. *Nat Commun.* 2022;13(1):4119.
15. Zhang KJ, Yin XF, Yang YQ, et al. A potent in vivo antitumor efficacy of novel recombinant type I interferon. *Clin Cancer Res.* 2017;23(8):2038–2049.
16. He TC, Zhou S, da Costa LT, et al. A simplified system for generating recombinant adenoviruses. *Proc Natl Acad Sci U S A.* 1998;95(5):2509–2514.
17. Fueyo J, Gomez-Manzano C, Alemany R, et al. A mutant oncolytic adenovirus targeting the Rb pathway produces anti-glioma effect in vivo. *Oncogene.* 2000;19(1):2–12.
18. Blair GE, Dixon SC, Griffiths SA, Zajdel ME. Restricted replication of human adenovirus type 5 in mouse cell lines. *Virus Res.* 1989;14(4):339–346.
19. Ying B, Toth K, Spencer JF, et al. INGN 007, an oncolytic adenovirus vector, replicates in Syrian hamsters but not mice: Comparison of biodistribution studies. *Cancer Gene Ther.* 2009;16(8):625–637.
20. Prescott J, Safronetz D, Haddock E, et al. The adaptive immune response does not influence hantavirus disease or persistence in the Syrian hamster. *Immunology.* 2013;140(2):168–178.
21. Prescott J, Falzarano D, Feldmann H. Natural immunity to ebola virus in the syrian hamster requires antibody responses. *J Infect Dis.* 2015;212(suppl 2):S271–S276.
22. Thomas MA, Spencer JF, La Regina MC, et al. Syrian hamster as a permissive immunocompetent animal model for the study of oncolytic adenovirus vectors. *Cancer Res.* 2006;66(3):1270–1276.
23. Wang G, Zhang Z, Zhong K, et al. CXCL11-armed oncolytic adenoviruses enhance CAR-T cell therapeutic efficacy and reprogram tumor microenvironment in glioblastoma. *Mol Ther.* 2023;31(1):134–153.
24. Wang G, Kang X, Chen KS, et al. An engineered oncolytic virus expressing PD-L1 inhibitors activates tumor neoantigen-specific T cell responses. *Nat Commun.* 2020;11(1):1395.
25. Liu W, Dai E, Liu Z, et al. In situ therapeutic cancer vaccination with an oncolytic virus expressing membrane-tethered IL-2. *Mol Ther Oncolytics.* 2020;17:350–360.

26. Ye K, Li F, Wang R, et al. An armed oncolytic virus enhances the efficacy of tumor-infiltrating lymphocyte therapy by converting tumors to artificial antigen-presenting cells in situ. *Mol Ther.* 2022;30(12):3658–3676.

27. Ma R, Lu T, Li Z, et al. An oncolytic virus expressing IL15/IL15Rα combined with off-the-shelf EGFR-CAR NK cells targets glioblastoma. *Cancer Res.* 2021;81(13):3635–3648.

28. Tian L, Xu B, Chen Y, et al. Specific targeting of glioblastoma with an oncolytic virus expressing a cetuximab-CCL5 fusion protein via innate and adaptive immunity. *Nat Cancer.* 2022;3(11):1318–1335.

29. Liu G-Y, Li Z-J, Li Q-L, et al. Enhanced growth suppression of TERT-positive tumor cells by oncolytic adenovirus armed with CCL20 and CD40L. *Int Immunopharmacol.* 2015;28(1):487–493.